International Journal for Housing Science and Its Applications
Publish August 10, 2025. Volume 46, Issue 4 Pages 7421-7437

https://doi.org/10.70517/ijhsa464642

Analysis of Multi-dimensional Factors Affecting Miners' Safety Awareness in Complex Construction and Mining Environments and Design of an Adaptive Assessment Model

Yan Zhang[1,2], Zhibo Yang[2], Xusheng Zhou[2] and Cody Ding[3,*]
[1] Safety Science and Engineering College, Liaoning Technical University, Fuxin, Liaoning, 123000, China
[2] School of Educational Science, Shenyang Normal University, Shenyang, Liaoning, 110000, China
[3] Department of Educational Psychology, University of Missouri-St, Louis, St.Louis, Missouri, 63121, USA

Corresponding authors: (e-mail: dingc@126.com).

Abstract Miners' safety awareness is crucial to mine safety production. Insufficient safety awareness among miners can easily lead to safety accidents. This study applies the DEMATEL-ISM model to explore the relationships among the multi-dimensional influencing factors of miners' safety awareness. First, a causal matrix and network relationship influence diagram for each dimension and indicator are constructed to identify 12 multi-dimensional influencing factors of miners' safety awareness and determine the key influencing factors. Second, based on a one-dimensional convolutional neural network, the SE-ResNetV2 model with a channel attention mechanism was constructed to achieve adaptive assessment of miners' safety vigilance. The DEMATEL-ISM model clearly reveals the hierarchical relationships among the factors influencing miners' safety vigilance, while the SE-ResNetV2 model reduces prediction errors to a certain extent. The relative prediction error of the model when inputting multi-dimensional data features is only 9.5%. This study provides new theoretical and technical pathways for ensuring safety in mine operations and has significant practical application value.

Index Terms DEMATEL-ISM model, SE-ResNetV2 model, channel attention factors influencing miner safety vigilance

I. Introduction

Coal accounts for a significant proportion of China's primary energy production and consumption structure, so it is essential to ensure the sustained, stable, and healthy development of the coal industry [1]. In recent years, China has experienced frequent coal mining accidents resulting in numerous fatalities. Although the government and coal mining companies have implemented a series of measures to prevent and control accidents in recent years, there remains a significant gap compared to developed countries [2], [3]. Humans are the central actors in coal mining operations, and unsafe human behavior and unsafe conditions of equipment are the primary causes of coal mine accidents, with human factors accounting for a high proportion [4]-[6]. Researching the influence of human factors on unsafe behavior from the perspective of human characteristics can play a positive role in preventing and reducing coal mine accidents [7], [8].

Alertness refers to the level of sustained attention or vigilance during task execution. Short-term fatigue and drowsiness are equivalent to alertness [9]. In coal mine accidents, unsafe behaviors and operational errors caused by reduced alertness levels—such as inattention and inappropriate reactions—among coal miners have led to numerous preventable accidents [10]-[12]. A higher alertness level can maintain miners' ability to anticipate dangers, enhance their safe and efficient operational capabilities, reduce accidents caused by human factors, and lower the incidence of coal mine safety accidents [13]-[15]. Therefore, the level of alertness among coal miners during operations is closely related to workplace safety. Employees with higher alertness levels are suitable for positions requiring prolonged concentration and prone to unsafe behaviors [16], [17].

Due to the poor working environment in construction mines, with high temperatures and humidity, and the generation of large amounts of coal dust and noise during operations, these factors severely impair human comfort and exacerbate physical exhaustion among miners [18]-[20]. These adverse environmental factors reduce miners' ability to concentrate and maintain alertness, making them highly susceptible to accidents caused by human factors and leading to coal mine production safety accidents [21], [22]. Therefore, studying the impact of employee alertness on unsafe behaviors and its relationship with physiological factors can help implement measures to assist employees in adjusting their state, enhancing alertness, and reducing the occurrence of unsafe behaviors, thereby contributing to the reduction of coal mine accidents [23]-[26].

Traditional scales and statistical analysis play a crucial role in assessing human alertness. Mahajan, K., et al. proposed using in-vehicle voice assistants to counteract the disengagement and fatigue effects caused by vehicle automation, and combined the Karolinska Sleepiness Scale to measure drivers' alertness, thereby evaluating the effectiveness of in-vehicle voice assistants [27]. Ferguson, B. A., et al. developed a 2-minute cognitive assessment tool and applied it to pre- and post-shift alertness assessments of emergency department residents, positively impacting shift scheduling and task allocation in the emergency department while identifying potential reductions in patient care errors due to physician fatigue [28]. Bihari, S., et al. used a scale data analysis method to examine fatigue, sleepiness, and behavioral alertness among intensive care unit (ICU) physicians, providing effective reference for ICU shift scheduling systems [29].

Domestic and international scholars have focused their research on alertness primarily on brainwave signals. Jiang, M., et al. developed an electroencephalogram (EEG) assessment tool to monitor changes in the cerebral cortex, combined with a machine learning framework to analyze drivers' alertness states under olfactory stimulation, and found that applying olfactory stimulation may be a potential strategy to regulate drivers' alertness [30]. Su, A. T., et al. used EEG testing methods to measure differences in brain rhythm spectral power before and after overnight shifts among doctors, while also combining the Chalder Fatigue Scale to survey information such as doctors' sleep duration. The proposed EEG screening and scale analysis tool can effectively detect mental fatigue among doctors [31]. Xavier, G et al. recorded EEG data from doctors before and after shifts, with differences in power in various brain regions serving as a quantitative measure of fatigue and alertness [32]. Di Flumeri, G et al. developed an alertness and attention controller for air traffic controllers using EEG and eye-tracking (ET) technology, which can automatically process and assess personnel alertness levels on duty [33].

Additionally, certain physiological signals can also serve as indicators of personnel alertness. Riani, K., et al. constructed a machine learning framework using multimodal driving session data, extracting multimodal features from session data to detect driver alertness, while also exploring differences between alertness and drowsiness [34]. Kumar, S., et al. proposed a driver alertness detection method based on physiological, environmental, and vehicle parameter indicators, whose excellent detection performance has made significant contributions to reducing traffic accident frequencies [35]. Li, Z., et al. investigated the application of biological signals in alertness prediction, proposing a benchmark testing framework for alertness prediction and feature analysis based on eye tracking, whose analysis results hold important reference value for traffic controllers' task execution [36]. Li, F. conducted a non-invasive analysis of traffic controllers' gaze patterns in both spatial and temporal contexts, thereby establishing an objective alertness assessment model that can effectively help traffic controllers avoid alertness reduction caused by fatigue [37]. Kouba, P., et al. believe that voice analysis can also accurately identify the fatigue state of on-duty personnel. Therefore, they proposed an alertness monitoring model based on hierarchical voice analysis (LVA) recognition technology, which can not only detect fatigue states from voice parameters but also monitor changes in personnel stress levels [38]. However, most of the above literature focuses on the alertness of drivers, doctors, and controllers during work, with few studies on the alertness of frontline coal workers. By analyzing the factors influencing miners' safety alertness and establishing a corresponding evaluation indicator system, it will be beneficial to enhance miners' judgment and response capabilities in complex work environments.

To improve the safety level of mining operations and reduce the risk of accidents in mines, this paper adopts a multi-dimensional approach, considering factors such as safety knowledge and skills, safety awareness, and safety behavior psychology. The DEMATEL-ISM model is used to construct a causal matrix and directed graph. Based on this, the SE-ResNetV2 model is integrated to construct an adaptive assessment model for miners' safety vigilance. This model utilizes a one-dimensional convolutional neural network to perform sliding window operations in a single direction, employing a more lightweight convolutional kernel size to extract a richer set of safety vigilance feature information. Experiments were designed to explore miner behavioral characteristics and alertness levels in complex construction and mining environments, as well as to validate the performance of the alertness prediction model, thereby verifying the effectiveness of the work presented in this paper.

II. Analysis of multi-dimensional factors affecting miners' safety awareness

II. A.DEMATEL-ISM Model

II. A. 1) Theoretical steps for DEMATEL-ISM model calculation

Step 1: Establish the initial direct influence matrix A. Calculate the arithmetic mean of the scores to obtain the initial direct influence matrix $A=[a_{ij}]_{n\times n}$ for each dimension and indicator. The three influence levels “0”, “1”, “2”, “3”, and “4” represent the following: Factor a_i has no influence on a_j, Factor a_i has a weak influence on a_j, Factor a_i has a moderate influence on a_j has a moderate influence, factor a_i has a strong influence on a_j, and factor a_i has a very strong influence on a_j.

$$A = \begin{bmatrix} a_{11} & \cdots & a_{1j} & \cdots & a_{1m} \\ \vdots & \vdots & \vdots & \vdots & \vdots \\ a_{i1} & \cdots & a_{ij} & \cdots & a_{im} \\ \vdots & \vdots & \vdots & \vdots & \vdots \\ a_{m1} & \cdots & \cdots & \cdots & a_{mm} \end{bmatrix} \tag{1}$$

Step 2: Establish a standardized direct impact matrix. To ensure the convergence of subsequent calculations, the initial direct impact matrix must be calculated using the following formula. The direct impact matrix can be normalized to obtain the following standardized direct impact matrix.

$$D = s \times A \tag{2}$$

$$s = \frac{1}{\max\limits_{1 \le i \le n} \sum\limits_{j=1}^{n} a_{ij}} \tag{3}$$

Step 3: Establish a comprehensive impact matrix. This step aims to further analyze the indirect impact relationships between various dimensions and indicators, which can be calculated using the following formula.

$$\begin{gathered} T = D + D^2 + D^3 + \cdots + D^h = D(I - D)^{-1} \\ \lim_{h \to \infty} D^h = [0]_{n \times n} \end{gathered} \tag{4}$$

Step 4: Draw a network relationship influence diagram for each dimension and indicator, and calculate the corresponding centrality and influence. The specific formulas for centrality and influence are as follows. Sum the formulas in each row and column of the comprehensive influence matrix and represent them with matrices r and c, respectively:

$$\begin{gathered} T = [t_{ij}], i, j = 1, 2, \cdots, n, \\ r = [r_i]_{n \times 1} = \left[\sum_{j=1}^{n} t_{ij} \right]_{n \times 1} \quad c = [c_j]_{n \times 1} = \left[\sum_{i=1}^{n} t_{ij} \right]_{n \times 1} \end{gathered} \tag{5}$$

r_i represents the sum of the i th row in the comprehensive influence matrix, i.e., the influence degree; c_j represents the sum of the j th column, i.e., the degree of influence. In the network relationship influence diagram, $X = r_i + c_j$ serves as the x-axis, with its value indicating the degree of centrality; while $Y = r_i + c_j$ serves as the y-axis, with its value indicating the degree of causality. If the value is positive, the indicator belongs to the cause group; otherwise, it belongs to the effect group.

ISM Steps: The Interpretive Structural Modeling (ISM) method [39] was developed as a method for analyzing issues related to complex socio-economic systems. Its characteristic is to decompose complex systems into several subsystems (or elements), utilize matrix calculation methods and the assistance of electronic computers, and ultimately construct a multi-level hierarchical structural model of the system. This model can transform vague ideas and perspectives into intuitive models with well-defined structural relationships.

This paper employs the ISM to establish the hierarchical relationships among the multidimensional influencing factors of miners' safety vigilance, thereby explaining the formation process of psychological crises. Based on the fundamental principles of the explanatory structural model, the matrix calculations of the explanatory structural model are employed to derive the explanatory structural model of the multidimensional influencing factors of miners' safety vigilance, providing a factual basis for the structural framework of influencing factors in intervention models. The schematic diagram of the explanatory structural model of the multidimensional influencing factors of miners' safety vigilance in the complex environment of construction mines is illustrated in Figure 1.

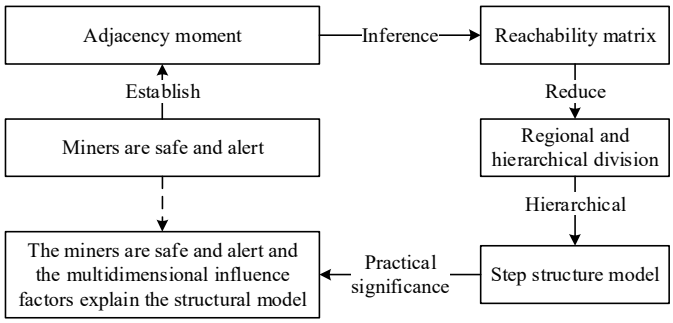

Figure 1: Interpretation structure model

Analyze the binary relationships among the constituent elements within the system by modeling the multidimensional influence factors affecting miner safety as a grid of n influence factors. The system is denoted as S, where $S=\{S_1,S_2,\cdots,S_n\}$ and (S_i,S_j) represents the ordered pair of elements S_i and S_j. All elements in the system S must be binary relationships.

Step 1: Construct the adjacency matrix. The adjacency matrix A is a square matrix that represents the binary relationships or direct connections between the elements of the system. If $A=(a_{ij})_{n\times n}$, then it is defined as:

$$\begin{cases}1, \text{If } i \text{ has an influence on } j\\ 0, \text{If } i \text{ has no influence on } j\end{cases} \tag{6}$$

Step 2: Establish an reachability matrix. Use Boolean algebra operations and matrix multiplication to obtain the reachability matrix R.

$$(A+I)\neq(A+I)^2\neq\cdots\neq(A+I)^{n-1}=(A+I)^n=R \tag{7}$$

Step 3: Establish a process network hierarchy diagram. Based on the reachability matrix R, divide the system elements associated with the elements $S_i(i=1,2,\ldots,n)$ into types and identify the elements with obvious characteristics in the entire system. The definition of the element set is as follows:

$$\begin{aligned}&a.\text{Reachable set } R(S_i)=\{S_j\mid S_j\in S, r_{ij}=1, j=1,2,\cdots,n\}, i=1,2,\cdots,n;\\ &b.\text{Antecedent set } A(S_i)=\{S_j\mid S_j\in S, r_{ji}=1, j=1,2,\cdots,n\}, i=1,2,\cdots,n;\\ &c.\text{Common set } C(S_i)=\{S_j\mid S_j\in S, r_{ij}=1, j=1,2,\cdots,n\}, i=1,2,\cdots,n;\end{aligned} \tag{8}$$

If there are elements in S that satisfy $R(S_i)=C(S_i)$ for all $S_i\in S$, then they are the highest elements. Remove them and find the remaining highest elements. Repeat this process until the lowest level element set is determined, completing the hierarchical structure diagram of the process network.

II. A. 2) DEMATEL and ISM Integration Model Structure

By introducing the intercept λ into the DEMATEL normalized influence matrix, statistical calculations are performed on the normalized influence matrix to obtain the results, where $\lambda=\bar{x}+\sigma$. The specific values should also be appropriately adjusted based on the hierarchical structure diagram. Values that are too large will result in too many levels, while values that are too small will result in only one level, thereby losing the significance of the study. Calculate the adjacency matrix A based on the normalized influence matrix:

$$\begin{cases}A_{ij}=1, t_{ij}\geq\lambda\\ A_{ij}=0, t_{ij}<\lambda\end{cases} \tag{9}$$

where $\bar{x}$ is the average value of the T matrix, and σ is the population standard deviation.

By integrating the DEMATEL and ISM models, the direct relationships between system elements are calculated into an adjacency matrix through the introduction of the intercept via the direct relationship influence matrix. Subsequently, the system explanatory structure model is obtained through matrix calculation and hierarchical reduction, thereby explaining and describing the key elements of the system. The structural analysis steps of the DEMATEL-ISM model [40] integration are shown in Figure 2.

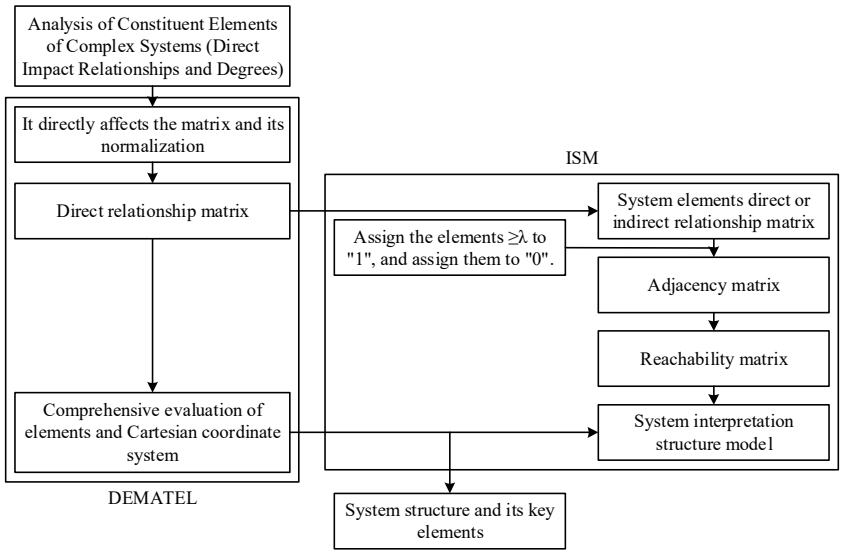

Figure 2: Integration structure diagram of the DEMATEL-ISM model

II. B.DEMATEL-ISM Model Construction and Analysis

II. B. 1) Construction of the DEMATEL-ISM Model

Identifying the multi-dimensional factors influencing safety awareness in complex construction mine environments, through interviews with miners in different positions, we have preliminarily identified the multi-dimensional factors influencing safety awareness in complex construction mine environments. Secondly, using the Delphi method, we invited eight experts in miner behavioral safety management (three professors, two associate professors, and three senior coal mine managers) to discuss the accuracy and independence of the factor descriptions. Based on simplified indicators and with the aim of ensuring that the meanings of the indicators do not overlap, 12 multidimensional factors influencing miners' safety vigilance were ultimately identified. The multidimensional factors influencing miners' safety vigilance in complex construction mine environments are shown in Table 1.

Table 1: Miners are safe and alert

Number	Formation factor	Number	Formation factor
A1	Safety knowledge skills	A7	Equipment and protection facilities
A2	Safety awareness	A8	Social exchange relations
A3	Psychology of safe behavior	A9	Working pressure
A4	Safe execution ability	A10	Safety supervision
A5	Safe mood	A11	Safety management
A6	Operating environment	A12	Safety education training

Based on the multi-dimensional influencing factors of miner safety awareness constructed according to Table 1, 10 experts in the field of miner behavior and psychological safety (5 from universities and 5 from coal mine enterprise management) were invited to evaluate the strength of interaction between the forming factors. The interaction strength was assigned values according to five levels: no influence (0 points), minor influence (1 point), moderate impact (2 points), significant impact (3 points), and very significant impact (4 points). This represents the degree of influence between each pair of formative factors, resulting in 10 initial direct influence matrices. To eliminate individual differences in expert scoring, the average of the 10 initial direct influence matrices was taken (rounded to the nearest integer), and a direct influence matrix for the multidimensional factors influencing miner safety vigilance was constructed.

The direct influence matrix is normalized using the row and maximum value method, yielding the standardized influence matrix. Calculating the standardized influence matrix yields the comprehensive influence matrix, as shown in Table 2. The largest value is 0.333 for A8-A12.

Table 2: Comprehensive influence matrix

F	A1	A2	A3	A4	A5	A6	A7	A8	A9	A10	A11	A12
A1	0.045	0.008	0.067	0.046	0.057	0.105	0.139	0.182	0.036	0.027	0.078	0.086
A2	0.081	0.016	0.038	0.054	0.070	0.194	0.189	0.144	0.083	0.144	0.184	0.058
A3	0.042	0.014	0.031	0.073	0.141	0.082	0.150	0.211	0.118	0.053	0.212	0.059
A4	0.033	0.009	0.025	0.044	0.123	0.047	0.024	0.197	0.075	0.186	0.203	0.059
A5	0.070	0.025	0.089	0.213	0.099	0.110	0.112	0.291	0.112	0.183	0.305	0.150
A6	0.111	0.012	0.034	0.056	0.127	0.042	0.139	0.199	0.040	0.050	0.153	0.056
A7	0.129	0.064	0.094	0.194	0.231	0.147	0.079	0.279	0.148	0.094	0.272	0.149
A8	0.146	0.048	0.071	0.084	0.091	0.058	0.051	0.111	0.051	0.046	0.183	0.144
A9	0.039	0.020	0.062	0.170	0.166	0.057	0.072	0.217	0.048	0.143	0.224	0.066
A10	0.040	0.021	0.040	0.050	0.049	0.150	0.037	0.122	0.042	0.034	0.219	0.139
A11	0.043	0.019	0.068	0.087	0.086	0.110	0.037	0.205	0.140	0.121	0.110	0.091
A12	0.181	0.092	0.168	0.204	0.218	0.161	0.132	0.333	0.195	0.143	0.290	0.090

The influence degree, affected degree, centrality, and causality of each forming factor were calculated. The DEMATEL calculation results are shown in Table 3. Among them, A8 has the highest centrality and A3 has the lowest centrality, with values of 3.575 and 1.603, respectively.

Table 3: Calculation results of DEMATEL

Factor	Influence degree	Influence degree	Center degree	Reason
A1	0.876	0.960	1.836	-0.084
A2	1.255	0.348	1.603	0.907
A3	1.186	0.787	1.973	0.399
A4	1.025	1.275	2.300	-0.250
A5	1.759	1.458	3.217	0.301
A6	1.019	1.263	2.282	-0.244
A7	1.880	1.161	3.041	0.719
A8	1.084	2.491	3.575	-1.407
A9	1.284	1.088	2.372	0.196
A10	0.943	1.224	2.167	-0.281
A11	1.117	2.433	3.550	-1.316
A12	2.207	1.147	3.354	1.060

Based on the centrality and causality values of each formative factor calculated in Table 3, Matlab software was used to plot a cause-and-effect diagram of the multidimensional influencing factors of miner safety awareness. The cause-and-effect diagram of the multidimensional influencing factors of miner safety awareness is shown in Figure 3.

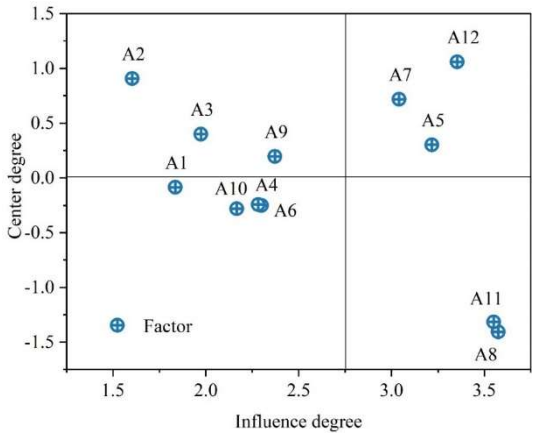

Figure 3: The reason for the safety of miners' safety vigilance: the result

By adding the identity matrix I to the comprehensive influence matrix in Table 3, we obtain the overall influence matrix. To derive the reachability matrix, a threshold λ is introduced to eliminate relationships with smaller influence.

Based on the cause-effect diagram and expert opinions, the paper sets λ to 0.14, 0.17, 0.20, and 0.23 to obtain node degree decay diagrams of the multidimensional influence factors affecting miners' safety awareness under different thresholds. The node degree decay diagram of the multidimensional influence factors of miner safety vigilance is shown in Figure 4. When λ is set to 0.20, the node degree is relatively moderate. Therefore, the threshold of 0.20 is selected in this paper. Based on the results of the overall influence matrix, the reachability matrix of the multidimensional influence factors of miner safety vigilance can be obtained. The reachability matrix of the multidimensional influence factors of miner safety vigilance is shown in Table 4.

Based on Table 4, the reachable set and leading set of the multi-dimensional influencing factors of miner safety vigilance can be calculated. After verification, when i = 1, 4, 6, 8, and 9, R(Ai) ∩ A(Ai) = R(Ai), and A1, A4, A6, A8, and A9 are the first-layer forming factors; By removing the rows and columns corresponding to these factors from the matrix and repeating the above steps, the second-level form factors A2 and A11 can be obtained. Similarly, the third-level form factors A3, A6, and A10; and the fourth-level form factors A7 and A12 can be obtained. Therefore, the multidimensional influencing factors of miner safety awareness can be divided into four levels, as shown in Figure 5.

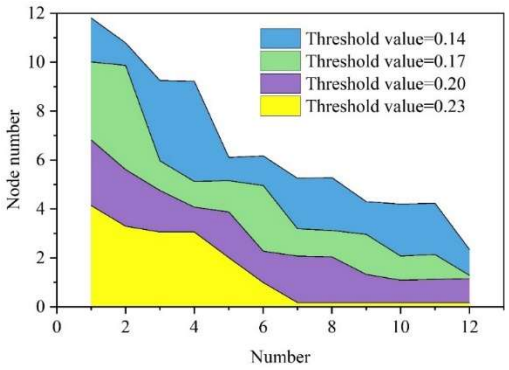

Figure 4: Scatter plot of node degree attenuation under different thresholds

Table 4: Calculation results of DEMATEL

F	A1	A2	A3	A4	A5	A6	A7	A8	A9	A10	A11	A12
A1	1	0	0	0	0	0	0	0	0	0	0	0
A2	0	1	0	0	0	0	0	0	0	0	0	0
A3	0	0	1	0	0	0	0	1	0	0	1	0
A4	0	0	0	1	0	0	0	0	0	0	1	0
A5	0	0	0	1	1	0	0	1	0	0	1	0
A6	0	0	0	0	0	1	0	0	0	0	0	0
A7	0	0	0	0	1	0	1	1	0	0	1	0
A8	0	0	0	0	0	0	0	1	0	0	0	0
A9	0	0	0	0	0	0	0	1	1	0	1	0
A10	0	0	0	0	0	0	0	0	0	1	1	0
A11	0	0	0	0	0	0	0	1	0	0	1	0
A12	0	0	0	1	1	0	0	1	0	0	1	1

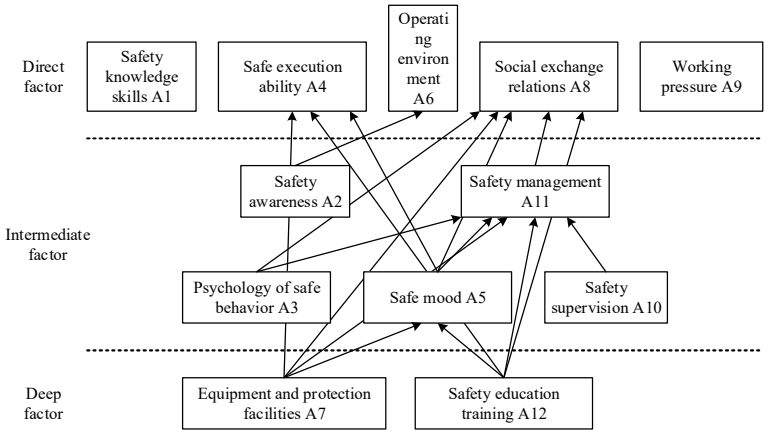

Figure 5: The formation factor of miners' unsafe sentiment ISM

II. B. 2) Analysis of Multidimensional Factors Affecting Miners' Safety Awareness

The causal relationships among the multidimensional influencing factors of miners' safety vigilance, as calculated by DEMATEL, reveal the following: The multidimensional influencing factors of miners' safety vigilance can be grouped into four categories. The first category is the strong causal factor set (Zone I), which has a very significant influence on the formation of miners' unsafe emotions and also exerts a considerable influence on other outcome-type factors; The second category is the weak causal factor set (Zone II), which also plays an important role in the formation of miners' safety vigilance awareness and has a certain influence on other outcome-type factors; The third category is the weak outcome factor set (Zone III), which is the result of the combined effects of other causal factors and has a certain influence on the formation of miners' safety vigilance awareness; The fourth category is the strong outcome factor set (Zone IV). These factors are also the result of the combined effects of other causal factors, but they have a very important influence on the formation of miners' safety awareness. The larger the factor centrality obtained through DEMATEL calculations, the greater the influence. Therefore, it is essential to focus on the strong causal factor set in Zone I and the strong result factor set in Zone IV. Based on centrality, the factors are ranked from highest to lowest influence as follows: social exchange relationships, safety management, safety education and training, safety emotions, and the condition of machinery, equipment, and protective facilities.

According to the ISM analysis results, the multidimensional influencing factors of miners' safety awareness exhibit complex relationships such as peer-level or cross-level connections. In this model, the multidimensional influencing factors of miners' safety awareness are divided into three major factor sets: direct factors (first level); intermediate factors (second and third levels); and deep-level factors (fourth level).

The condition of machinery, equipment, and protective facilities (A7) and safety education and training (A12) are deeper-level factors influencing the formation of miners' safety vigilance awareness.

Safety awareness (A2), safety management (A11), safety behavioral psychology (A3), safety emotions (A5), and safety supervision (A10) belong to the second and third levels of the ISM model and are intermediate factors influencing the formation of miners' safety vigilance awareness.

Safety knowledge and skills (A1), safety execution ability (A4), work environment (A6), social exchange relationships (A8), and work pressure (A9) are direct factors in the formation of miners' safety awareness.

In the ISM model, factors with higher node degrees include Machine Equipment and Protective Facilities Condition (A7), Safety Education and Training (A12), Safety Emotions (A5), Safety Management (A11), Social Exchange Relationships (A8), and Safety Execution Capability (A4). These factors are largely consistent with those identified through DEMATEL analysis as having higher centrality values and require particular attention.

II. C.Study on Miner Behavior Characteristics and Alertness Levels

II. C. 1) Experimental Design

Design an experiment to characterize miner behavior, complete subjective questionnaires, record behavioral data, analyze changes in miner work behavior characteristics, evaluate miner alertness levels, identify trends in alertness level changes, develop scientifically sound work schedules and rest systems, provide appropriate stimuli to enhance alertness levels, improve miner work reliability, and ensure the safe and normal operation of the cage. A combination of objective and subjective methods was used to design and evaluate an alertness experiment for miners in the auxiliary shaft.

The total sample size of mine workers in the auxiliary shaft is relatively small, typically fewer than 20 individuals. Considering the experimental objectives, participants with over five years of work experience and and those with proficient operational skills as the research subjects. Since the EEG electrodes must be in close contact with the subject's scalp to ensure signal quality, subjects with shorter hair and no history of neurological disorders were selected. Ultimately, 10 miners were chosen as research subjects, which to some extent meets the basic requirements for statistical analysis.

II. C. 2) Subjective Scale Analysis

The entire formal experimental process consisted of nine experiments, with a 20-minute interval between each experiment. Experiment 1 was the initial state, i.e., the alertness test before the task. During each experiment, the miners filled out the Karolinska Subjective Questionnaire, and the final results were the scores of nine experiments conducted on 10 miners within 180 minutes, as shown in Table 5.

Table 5: score table of subjective evaluation

Trial number	Experimental stage								
	1	2	3	4	5	6	7	8	9
1	4	4	3	3	5	6	7	7	8
2	4	4	3	3	5	5	7	8	8
3	4	3	3	3	5	5	7	8	8
4	4	4	3	4	4	6	7	7	9
5	5	4	2	3	5	6	7	8	8
6	5	4	3	4	5	6	7	8	9
7	4	5	3	3	5	6	6	8	7
8	4	4	3	4	4	6	7	8	9
9	4	4	2	3	5	6	6	8	8
10	4	4	3	3	5	6	7	7	8
Mean	4.2	4.0	2.8	3.3	4.8	5.8	6.8	7.7	8.2

Based on the average KSS scores of the miners, a trend chart of subjective score changes was plotted. The trend chart of subjective score changes is shown in Figure 6. Among them, Experiment 1 was the control experiment, i.e., the results obtained when the miners were well-prepared for work. Experiments 2 to 9 were conducted once every 20 minutes of work.

As the miners worked and the experiments progressed, the average KSS subjective scores first decreased and then increased, reflecting that the miners' alertness levels first increased and then decreased. The highest rate of change occurred between Experiment 4 and Experiment 5, indicating that during this phase, the miners' alertness levels decreased most rapidly. At the beginning of the experiment, i.e., Experiment 1, most miners scored 4 points on the KSS scale, indicating that they were at a general alertness level. In Experiment 3, most miners scored 3 points, indicating they were in an alert state, with the highest alertness levels at this point. After 180 minutes of work, i.e., Experiment 9, miners achieved the highest KSS scores, mostly 8 points, indicating they were in a fatigued state, requiring effort to maintain alertness. There were significant differences between Experiment 1, Experiment 3, and Experiment 9, with KSS subjective scores of 4.2, 2.8, and 8.2, respectively. To determine whether the score differences between Experiment 1 and Experiment 3, and between Experiment 3 and Experiment 9, were significant, a paired samples t-test was used to analyze the differences between the experimental results, as the data came from the same group of miners. The prerequisite for a paired t-test is that the samples follow a normal distribution. In SPSS, we tested whether the differences in mean scores between Experiment 3 and Experiment 1 (d1, Experiment 3 - Experiment 1) and between Experiment 9 and Experiment 3 (d2, Experiment 9 - Experiment 3) followed a normal distribution. The test results are shown in Table 6.

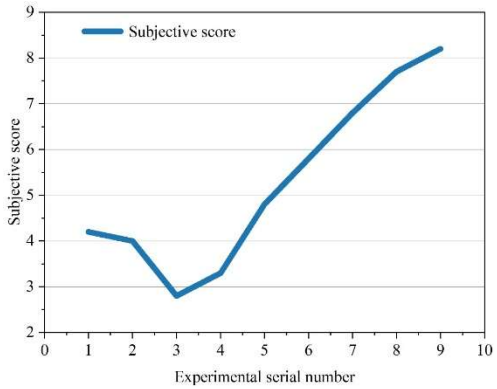

Figure 6: Variation trend of subjective mean score

Table 6: Normality test

	Kormogov smealov (V)[a]			Shapiro wilk		
	Statistics	Freedom	Significance	Statistics	Freedom	Significance
d1	0.332	10	0.002	0.652	10	0.000
d2	0.484	10	0.000	0.480	10	0.000

Due to the small sample size, the Shapiro-Wilk test was selected. The results showed that the significance level P-values were all less than 0.05, indicating that the sample differences did not follow a normal distribution. Therefore, the paired samples t-test could not be performed, and the nonparametric rank sum test was selected instead. The test results are shown in Table 7.

During the period from Experiment 1 to Experiment 3, i.e., from 0 to 60 minutes, the miners' subjective alertness levels continued to increase. At this stage, the nonparametric test yielded a significance level P = 0.003 < 0.05, indicating a significant difference between the two groups of samples; From Experiment 3 to Experiment 9, i.e., between 40 and 180 minutes, the miners' subjective alertness levels decreased. At this point, the nonparametric test significance level P = 0.002 < 0.05, indicating a significant difference. Therefore, the alertness levels of the miners in Experiment 1 and Experiment 3, as well as Experiment 3 and Experiment 9, were in different states.

Table 7: KSS score non-parametric test

	Experiment 3- experiment 1	Experiment 9-experiment 3
Z	-3.144[b]	-3.272[c]
Asymptotically significant (double tail)	0.003	0.002

II. C. 3) Reaction capability test

Using a reaction time test program, the reaction time of miners to target signals was recorded. Due to the low difficulty of the experimental design, the correct response rate of the test miners remained above 98%. The mean reaction time of the miners was selected as the task performance metric to assess changes in alertness as working hours increased. The reaction times of the miners during the experiment are shown in Table 8.

Table 8: Reaction time(ms)

Trial number	Experimental stage								
	1	2	3	4	5	6	7	8	9
1	1134.0	999.6	918.3	965.6	1087.9	1248.3	1330.3	1364.1	1496.8
2	1068.6	1034.2	915.3	966.5	1126.4	1267.7	1361.5	1359.0	1429.1
3	1081.1	1090.4	940.9	958.6	1154.8	1242.6	1286.5	1278.2	1485.5
4	1075.4	1006.7	958.9	925.8	1085.6	1317.2	1370.7	1303.9	1476.5
5	1088.9	1054.9	922.5	951.6	1059.0	1191.1	1315.3	1352.1	1349.8
6	1043.7	1068.4	924.1	999.1	1168.9	1173.9	1310.6	1405.5	1514.4
7	1008.3	1044.0	902.7	944.7	1185.0	1192.6	1346.9	1320.7	1517.2
8	1095.7	1090.1	892.4	918.3	1084.1	1177.3	1361.3	1437.1	1451.3

9	1147.0	1033.0	939.0	956.7	1159.0	1284.6	1290.0	1350.8	1405.2
10	1105.0	981.2	873.1	907.9	1134.3	1244.5	1292.6	1490.4	1460.5
Mean	1084.77	1040.25	918.72	949.48	1124.50	1233.98	1326.57	1366.18	1458.63

Based on the average reaction time data in Table 8, a graph showing the changes in the average reaction time of miners across different experimental stages was plotted. The changes in the average reaction time of miners are shown in Figure 7. From Experiment 1 to Experiment 3, the average reaction time of miners continued to decrease. From Experiment 3 to Experiment 9, the average reaction time increased continuously. Regarding the subjective division and flash fusion frequency, a normality test was first conducted on the reaction time differences. The results of the normality test are shown in Table 9. For d3, $p = 0.346 > 0.05$, indicating normality, and for d4, $p = 0.758 > 0.05$, also indicating normality. Therefore, a paired t-test was selected. The results of the paired t-test for reaction time are shown in Table 10.

As task duration increases, the trend in miners' reaction times is first to decrease and then increase, indicating that miners' ability to respond to signals first improves and then deteriorates, i.e., miners' alertness first increases and then decreases. Additionally, the differences in reaction times between experiments are significant, indicating that changes in miners' alertness are pronounced.

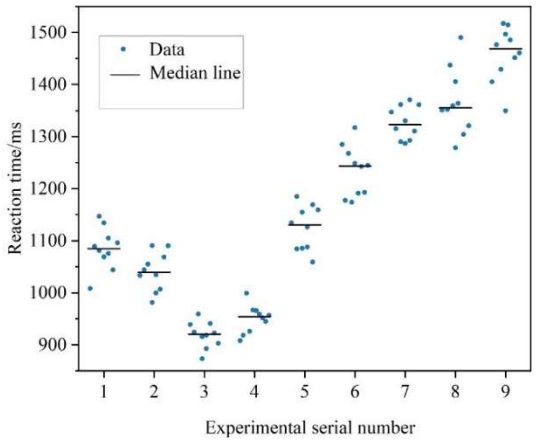

Figure 7: Reaction time diagram

Table 9: Reaction time normality test

	Kormogov smealov (V)[a]			Shapiro wilk		
	Statistics	Freedom	Significance	Statistics	Freedom	Significance
d3	0.125	10	0.2	0.925	10	0.346
d4	0.133	10	0.2	0.955	10	0.758

Table 10: Reaction time paired T-test

	Mean value	Standard deviation	Standard error mean	The difference is 95% of the confidence interval	The difference is 95% true interval limit	t	Freedom	Sig.2
Experiment 3-experiment 1	187.12	65.13	18.82	146.18	227.75	9.92	9	0.000
Experiment 9-experiment 3	-538.26	54.24	15.64	-572.81	-503.11	-34.26	9	0.000

III. Adaptive assessment model for miner safety awareness based on deep learning

III. A. Convolutional Neural Networks

III. A. 1) Overview of Convolutional Neural Networks

The classic convolutional model LeNet-5 [41], based on the gradient backpropagation algorithm, marked the beginning of the rapid development of convolutional neural networks (CNNs). The classic LeNet-5 model structure successfully achieved accurate recognition of handwritten digits. Convolutional neural networks are end-to-end networks that allow weights to be shared across different positions. Compared to traditional feedforward neural networks of similar network scale, convolutional neural networks have fewer connections and parameters, making model training easier. A typical CNN primarily consists of one or more convolutional layers, pooling layers, fully connected layers, and a final output layer.

III. A. 2) Activation function

The activation function of a neural network can increase the nonlinear expression capability of input data and enhance the network's learning of complex features in the data. It is the core of a neuron and even the entire neural network. Common activation functions include the sigmoid function, the tanh function, and the ReLU function.

(1) The mathematical expression of the sigmoid function is:

$$sigmoid(x) = \frac{1}{1+e^{-x}} \tag{10}$$

According to the mathematical expression, the output range of the sigmoid function is between 0 and 1, which is suitable for use as the output of a binary classification model for predicting probabilities.

(2) The mathematical expression of the tanh function is:

$$\tanh(x) = \frac{e^{x}-e^{-x}}{e^{x}+e^{-x}} \tag{11}$$

The output range of the tanh function is between -1 and 1. The tanh function is similar to the sigmoid function but solves the problem of the sigmoid function not having a zero mean output. When features differ significantly, using the tanh activation function can continuously amplify the feature effect, and it is often used as the activation function for the hidden layer of neural networks. However, it also suffers from the problem of gradient vanishing.

(3) The mathematical expression of the ReLU function is

$$\mathrm{Re}\,LU(x) = \begin{cases} \max(x,0), x >= 0 \\ 0, x < 0 \end{cases} \tag{12}$$

The ReLU function is one of the most commonly used activation functions in deep learning. The ReLU function has a reciprocal value of 1 in the positive interval and does not saturate, which can accelerate the convergence speed of gradient descent and effectively alleviate the problems of gradient disappearance and gradient explosion.

III. A. 3) Loss Function

The choice of loss function has a significant impact on the final performance of the model and should be selected appropriately based on the model type.

(1) Regression problems

The mean squared error (MSE) loss function, also known as the L2 loss function, represents the average of the squared differences between the predicted values and the actual values. It is a commonly used loss function in regression problems. The mathematical expression is shown below:

$$MSE = L2 = \frac{1}{N}\sum_{i=1}^{N}(y_i - \hat{y}_i)^2 \tag{13}$$

In the equation, N represents the number of samples, y_i represents the true value of the sample, and $\hat{y}_i$ represents the predicted value of the model.

The mean absolute error (MAE) is also known as the L1 loss function and can similarly be used as the loss function for a regression model. The mathematical expression represents the sum of the absolute differences between the predicted values and the actual values. It has a stable gradient for any input value and does not cause gradient explosion issues.

$$MAE = L1 = \frac{1}{N}\sum_{i=1}^{N}| y_i - \hat{y}_i | \tag{14}$$

In the equation, N represents the number of samples, y_i represents the true value of the sample, and $\hat{y}_i$ represents the predicted value of the model.

(2) Classification problems

The cross-entropy loss function is used to evaluate the difference between the probability distribution of the actual output and the true probability distribution, and is commonly used in classification problems. The mathematical expression for the cross-entropy loss function based on a binary classification problem is:

$$L = \frac{1}{N}\sum_{i=1}^{N} -[y_i \log(p_i) + (1-y_i)\log(1-p_i)] \tag{15}$$

In the formula, N denotes the number of samples, γ_i denotes the sample label, with positive class being 1 and negative class being 0, and p_i denotes the probability of the model predicting a positive class. The cross-entropy function is used as the loss function for the miner alertness classification model in this paper.

III. A. 4) Optimization Methods

The loss function defines the degree of difference between the predicted value of the current network output and the target value. To ensure the accuracy of the model's predictions, optimization algorithms are used to iteratively find the minimum value of the loss function and its corresponding parameters.

(1) Gradient descent method

The gradient descent method involves continuously calculating the gradient value during the iteration process and calculating the forward step length according to the learning rate η. The weight value W is continuously adjusted in the opposite direction of the gradient of the given point so that the value of the loss function becomes smaller and smaller, eventually reaching the lowest point of the loss function. The mathematical description is as follows:

$$W = W - \eta\frac{\partial L}{\partial W} \tag{16}$$

In the formula, η represents the learning rate, i.e., the step size of each gradient descent.

(2) Momentum algorithm

Momentum is an optimization of the gradient descent method. It uses the concept of “momentum” to describe changes in movement trends. When parameters are updated, the current update speed is accelerated by accumulating the momentum from previous updates, which allows the network to converge more optimally and stably and reduces oscillations. Its mathematical description is as follows:

$$\begin{cases} v = \alpha v - \eta\dfrac{\partial L}{\partial W} \\ W = W + v \end{cases} \tag{17}$$

In the equation, α represents the momentum parameter, and υ represents the accumulated momentum sum.

(3) Adam algorithm

The Adam algorithm uses first-order and second-order moment estimates to determine the model gradient update direction and learning rate update adjustment, respectively, and accelerates convergence speed through momentum and adaptive learning rates.

$$\begin{cases} \upsilon = \alpha\upsilon + (1-\alpha)\dfrac{\partial L}{\partial W} \\ h = \rho h + (1-\rho)(\dfrac{\partial L}{\partial W})^2 \\ W = W - \dfrac{\eta}{\sqrt{h}} * \upsilon \end{cases} \tag{18}$$

In the equation, α represents the momentum parameter, υ represents the accumulated momentum sum, h represents the accumulated squared gradient, and ρ represents the gradient accumulation exponent.

The Adam algorithm is suitable for solving optimization problems involving large-scale data and parameters, as well as problems with high noise or sparse gradients. Additionally, the Adam algorithm is insensitive to the learning rate and performs exceptionally well in current practical parameter tuning, making it widely used in the field of deep learning.

III. B. Model construction based on one-dimensional convolutional neural networks

(1) ResNet Model

Depending on the complexity of the extracted features, the ResNet model [42] can flexibly set different numbers of network layers to concatenate residual modules, thereby improving the efficiency of deep networks. Compared to the VGG network, the ResNet uses fewer data parameters and trains faster. Since physiological signal features are relatively fewer than those in the image domain, this paper improves and constructs a miner alertness detection model based on the ResNet-18 network block.

(2) SENet model

Since the collected EEG, ECG, and EMG signals are human bioelectric signals containing a wealth of information about human physiological functions, it is essential to focus on extracting and training features related to fatigue states during alertness detection. This paper enhances the detection performance of the model by adding an SE module with channel attention mechanisms to the ResNet network.

The SE module is embedded into the ResNet model, and feature re-calibration is performed on the residual blocks of the branches before the Addition operation. The improved SE-ResNetV2 model is used, and one-dimensional convolution is employed for computation due to the special nature of physiological signals.

III. C. Alertness Adaptive Assessment Model Prediction Results

To investigate the impact of the temporal characteristics of miners' alertness features on model prediction performance, when constructing the SE-ResNetV2 model based on the channel attention mechanism, sequence features with temporal lengths ranging from 1 to 10 were input. The model performance when inputting different temporal sequence lengths is shown in Table 11. When the temporal sequence length of the alertness features was 5, the model achieved the best prediction performance. During the experiment, the reaction time of miners to signal stimuli ranged from 730 to 1350 ms, with an average reaction time of 966.12 ms. The mean nMAE and nRMSE values for the model's prediction of driver reaction time were 92.84 and 102.36 ms, respectively, with a relative prediction error of 9.7%. When the input features were single-point samples, the mean nMAE and nRMSE of the model were 110.45 and 136.52 ms, respectively. As the length of the input time series increased, the prediction performance of the model improved significantly, reaching the best prediction effect when the sequence length was 5. The results indicate that utilizing driver alertness features at the temporal level can effectively improve the SE-ResNetV2 model's prediction accuracy for miner reaction times. However, as the time series length continues to increase, the model's performance shows a slight decline, possibly due to the inclusion of redundant information in overly long time series features, which affects the accuracy of the miner alertness prediction model.

Table 11: Model performance of the length k in different time series

k	nMAE/ms	nRMSE/ms	nMRE/%
1	110.45(±18.11)	136.52(±24.33)	11.5
2	106.75(±22.64)	131.22(±25.12)	11.2
3	101.92(±18.29)	124.41(±17.44)	10.8
4	96.04(±16.64)	113.64(±14.16)	10.0
5	92.84(±13.44)	102.36(±12.12)	9.7
6	95.42(±12.84)	108.61(±14.05)	9.9
7	98.11(±14.47)	111.85(±15.03)	10.2
8	97.62(±15.55)	109.72(±13.62)	10.2
9	98.93(±13.31)	110.06(±14.58)	10.3
10	100.02(±15.74)	114.26(±16.51)	10.5

To further analyze the performance of the model and the impact of the attention mechanism on the model's predictive ability, miner alertness features with a time series length of 5 were input into the LSTM, SVR, LSSVM, and SE-ResNetV2 models for comparison. The model prediction performance comparison is shown in Table 12. The prediction accuracy of LSTM is significantly higher than that of SVR and LSSVM, indicating that LSTM has stronger adaptability when processing miner alertness time series features. On the other hand, the introduction of

the attention mechanism reduced the nMAE of the SE-ResNetV2 model by approximately 6% and the nRMSE by approximately 8%. This indicates that the attention mechanism helps extract the temporal characteristics of the association between miners' modal features and alertness, further improving the model's predictive accuracy for miners' reaction times.

Table 12: Model predictability can be compared

Model	nMAE/ms	nRMSE/ms	nMRE/%
LSTM	98.67(±17.28)	110.86(±15.63)	10.3
SVR	105.25(±18.71)	114.52(±16.15)	10.8
LSSVM	102.05(±17.75)	115.48(±16.24)	10.5
SE-ResNetV2	92.84(±13.48)	102.32(±12.12)	9.5

Eye movement features, electrocardiogram (ECG) features, and line parameters were sequentially input into the SE-ResNetV2 model to investigate the impact of different modal features on model performance. The effects of input modalities on model performance are summarized in Table 13. When considering single physiological features, using eye movement features to predict miners' reaction times yielded better results than using ECG features. Compared to using only eye movement features as input, the addition of ECG features reduced the model's nMAE from 98.98 ms to 93.28 ms and the nRMSE from 123.49 ms to 104.64 ms. The results indicate that integrating physiological features from both modalities can describe miners' alertness levels from different perspectives, thereby improving the model's prediction accuracy for reaction times. Additionally, the line environment is one of the factors considered in this paper that influences changes in miners' alertness levels. When line features and miners' physiological features are input into the model together, the model's predictive capability further improves, with the model's average nMAE and nRMSE for predicting miners' reaction times being 92.86 and 102.31 ms, respectively, and the model's relative error being 9.5%.

Table 13: The effect of model input modal model performance

Input signal	nMAE/ms	nRMSE/ms	nMRE/%
Eye movement	98.95(±15.74)	123.49(±19.01)	10.3
Cardiac power	108.92(±14.32)	133.93(±17.43)	11.2
Heart power + eye movement	93.27(±11.05)	104.64(±14.27)	9.8
Heart power + eye movement + line environment	92.85(±13.44)	102.31(±12.12)	9.5

IV. Conclusion

This paper employs the DEMATEL-ISM model to conduct an in-depth exploration of the multi-dimensional influencing factors of miners' safety vigilance in the complex environment of construction mining sites. Additionally, it constructs an adaptive vigilance assessment model based on SE-ResNetV2.

Through the application of the DEMATEL-ISM model, numerous factors are reasonably categorized into hierarchical levels based on their importance and degree of interaction. The study finds that the condition of machinery and protective facilities (A7), safety education and training (A12), safety emotions (A5), safety management (A11), social exchange relationships (A8), and safety execution capabilities (A4) have a significant impact on the formation of miners' safety vigilance awareness in complex construction mining environments. This helps enterprises formulate more effective safety training and management strategies to reduce the probability of mine safety accidents.

In terms of miner vigilance adaptive assessment, the introduction of the attention mechanism in this model reduces the nMAE and nRMSE of miner vigilance adaptive prediction by more than 5%. The input of line features and miners' physiological features further enhances the model's alertness prediction capability, with a relative prediction error of only 9.5%, indicating that the model can efficiently process miners' physiological signal data, improving prediction accuracy and stability, and providing reliable technical support for mine safety management.

References

[1] Li, X., Cao, Z., & Xu, Y. (2025). Characteristics and trends of coal mine safety development. Energy Sources, Part A: Recovery, Utilization, and Environmental Effects, 47(1), 2316-2334.

[2] Tian, J., Wang, Y., & Gao, S. (2022). Analysis of mining-related injuries in Chinese coal mines and related risk factors: A statistical research study based on a meta-analysis. International Journal of Environmental Research and Public Health, 19(23), 16249.

[3] Duarte, J., Baptista, J. S., & Torres Marques, A. (2019). Occupational accidents in the mining industry—a short review. Occupational and Environmental Safety and Health, 61-69.
[4] Niu, L., & Zhao, R. (2022). The effect of safety attitudes on coal miners' human errors: A moderated mediation model. Sustainability, 14(16), 9917.
[5] Liu, R., Cheng, W., Yu, Y., & Xu, Q. (2018). Human factors analysis of major coal mine accidents in China based on the HFACS-CM model and AHP method. International journal of industrial ergonomics, 68, 270-279.
[6] Zhang, M., Li, H., Xia, H., Zhang, Q., Chen, Y., Liu, Y., & Xu, H. (2024). Human factors analysis of coal mine gas accidents based on improved HFACS model. Human Factors and Ergonomics in Manufacturing & Service Industries, 34(4), 309-324.
[7] Feng, Y., Chen, H., Zhang, Y., & Jing, L. (2019). The hybrid systems method integrating human factors analysis and classification system and grey relational analysis for the analysis of major coal mining accidents. Systems Research and Behavioral Science, 36(4), 564-579.
[8] Fu, G., Xie, X., Jia, Q., Tong, W., & Ge, Y. (2020). Accidents analysis and prevention of coal and gas outburst: Understanding human errors in accidents. Process safety and environmental protection, 134, 1-23.
[9] Chandrakumar, D., Keage, H. A., Gutteridge, D., Dorrian, J., Banks, S., & Loetscher, T. (2019). Interactions between spatial attention and alertness in healthy adults: a meta-analysis. Cortex, 119, 61-73.
[10] Warm, J. S., Matthews, G., & Finomore Jr, V. S. (2018). Vigilance, workload, and stress. In Performance under stress (pp. 131-158). CRC Press.
[11] Dillard, M. B., Warm, J. S., Funke, G. J., Nelson, W. T., Finomore, V. S., McClernon, C. K., ... & Funke, M. E. (2019). Vigilance tasks: Unpleasant, mentally demanding, and stressful even when time flies. Human factors, 61(2), 225-242.
[12] Bauerle, T., Dugdale, Z., & Poplin, G. (2018). Mineworker fatigue: A review of what we know and future decisions. Mining engineering, 70(3), 33.
[13] Hébert, M., Lavigne, A. A., Auclair, J., Martin, J. S., Francis, K., Gagnon, J. D., ... & Laberge, L. (2023). A blue-enriched light intervention counteracts the alertness decrement among mine workers on extended 12-hour night shift periods. Journal of Occupational and Environmental Medicine, 65(7), 584-589.
[14] Dugdale, Z., Eiter, B., Chaumont Menendez, C., Wong, I., & Bauerle, T. (2022). Findings from a systematic review of fatigue interventions: What's (not) being tested in mining and other industrial environments. American journal of industrial medicine, 65(4), 248-261.
[15] Legault, G., Clement, A., Kenny, G. P., Hardcastle, S., & Keller, N. (2017). Cognitive consequences of sleep deprivation, shiftwork, and heat exposure for underground miners. Applied ergonomics, 58, 144-150.
[16] Maisey, G., Cattani, M., Devine, A., Lo, J., & Dunican, I. C. (2021). The sleep of shift workers in a remote mining operation: methodology for a randomized control trial to determine evidence-based interventions. Frontiers in neuroscience, 14, 579668.
[17] Drews, F. A., Rogers, W. P., Talebi, E., & Lee, S. (2020). The experience and management of fatigue: a study of mine haulage operators. Mining, Metallurgy & Exploration, 37, 1837-1846.
[18] Pan, H., Tong, S., Song, H., & Chu, X. (2025). A miner mental state evaluation scheme with decision level fusion based on multidomain EEG information. IEEE Transactions on Human-Machine Systems.
[19] Chen, S., Xu, K., Yao, X., Zhu, S., Zhang, B., Zhou, H., ... & Zhao, B. (2021). Psychophysiological data-driven multi-feature information fusion and recognition of miner fatigue in high-altitude and cold areas. Computers in biology and medicine, 133, 104413.
[20] Xu, L., Li, J., & Feng, D. (2023). Miner fatigue detection from electroencephalogram-based relative power spectral topography using convolutional neural network. Sensors, 23(22), 9055.
[21] Talebi, E., Rogers, W. P., Morgan, T., & Drews, F. A. (2021). Modeling mine workforce fatigue: Finding leading indicators of fatigue in operational data sets. Minerals, 11(6), 621.
[22] Tian, F., Li, H., Tian, S., Shao, J., & Tian, C. (2022). Effect of shift work on cognitive function in Chinese coal mine workers: a resting-state fNIRS study. International Journal of Environmental Research and Public Health, 19(7), 4217.
[23] OMIDI, L., ZARE, S., RAD, R. M., MESHKANI, M., & KALANTARY, S. (2017). Effects of shift work on health and satisfaction of workers in the mining industry. International journal of occupational hygiene, 9(1), 21-25.
[24] Li, J., Qin, Y., Guan, C., Xin, Y., Wang, Z., & Qi, R. (2022). Lighting for work: a study on the effect of underground low-light environment on miners' physiology. Environmental Science and Pollution Research, 1-10.
[25] Kuang, Y., Tian, S., Li, H., Yuan, C., & Chen, L. (2025). EEG-Based Measurement for Detecting Distraction in Coal Mine Workers. Applied Sciences (2076-3417), 15(1).
[26] Bajaj, V., Taran, S., Khare, S. K., & Sengur, A. (2020). Feature extraction method for classification of alertness and drowsiness states EEG signals. Applied Acoustics, 163, 107224.
[27] Mahajan, K., Large, D. R., Burnett, G., & Velaga, N. R. (2021). Exploring the effectiveness of a digital voice assistant to maintain driver alertness in partially automated vehicles. Traffic injury prevention, 22(5), 378-383.
[28] Ferguson, B. A., Lauriski, D. R., Huecker, M., Wichmann, M., Shreffler, J., & Shoff, H. (2020). Testing alertness of emergency physicians: a novel quantitative measure of alertness and implications for worker and patient care. The Journal of emergency medicine, 58(3), 514-519.
[29] Bihari, S., Venkatapathy, A., Prakash, S., Everest, E., McEvoy R, D., & Bersten, A. (2020). ICU shift related effects on sleep, fatigue and alertness levels. Occupational medicine, 70(2), 107-112.
[30] Jiang, M., Chaichanasittikarn, O., Seet, M., Ng, D., Vyas, R., Saini, G., & Dragomir, A. (2024). Modulating driver alertness via ambient olfactory stimulation: a wearable electroencephalography study. Sensors, 24(4), 1203.
[31] Su, A. T., Xavier, G., & Kuan, J. W. (2023). The measurement of mental fatigue following an overnight on-call duty among doctors using electroencephalogram. Plos one, 18(7), e0287999.
[32] Xavier, G., Su Ting, A., & Fauzan, N. (2020). Exploratory study of brain waves and corresponding brain regions of fatigue on-call doctors using quantitative electroencephalogram. Journal of occupational health, 62(1), e12121.
[33] Di Flumeri, G., De Crescenzio, F., Berberian, B., Ohneiser, O., Kramer, J., Aricò, P., ... & Piastra, S. (2019). Brain–computer interface-based adaptive automation to prevent out-of-the-loop phenomenon in air traffic controllers dealing with highly automated systems. Frontiers in human neuroscience, 13, 296.
[34] Riani, K., Papakostas, M., Kokash, H., Abouelenien, M., Burzo, M., & Mihalcea, R. (2020, June). Towards detecting levels of alertness in drivers using multiple modalities. In Proceedings of the 13th ACM International Conference on PErvasive Technologies Related to Assistive Environments (pp. 1-9).

[35] Kumar, S., Kalia, A., & Sharma, A. (2017, December). Predictive analysis of alertness related features for driver drowsiness detection. In International conference on intelligent systems design and applications (pp. 368-377). Cham: Springer International Publishing.
[36] Li, Z., Li, R., Yuan, L., Cui, J., & Li, F. (2024). A benchmarking framework for eye-tracking-based vigilance prediction of vessel traffic controllers. Engineering Applications of Artificial Intelligence, 129, 107660.
[37] Li, F., Chen, C. H., Lee, C. H., & Feng, S. (2022). Artificial intelligence-enabled non-intrusive vigilance assessment approach to reducing traffic controller's human errors. Knowledge-Based Systems, 239, 108047.
[38] Kouba, P., Šmotek, M., Tichý, T., & Kopřivová, J. (2023). Detection of air traffic controllers' fatigue using voice analysis-An EEG validation study. International Journal of Industrial Ergonomics, 95, 103442.
[39] Rakesh Kumar & Vinay Kandpal. (2025). Factors affecting the adoption of industry 4.0 technologies in circular economy: interpretive structure modelling (ISM) approach for future sustainability. Discover Sustainability,6(1),351-351.
[40] Jian Kang,Han Wang,Hao Jin,Zhixing Wang & Jixin Zhang. (2025). Risk analysis and management of hydrogen station fire and explosion accidents using DEMATEL-ISM and complex network models. International Journal of Hydrogen Energy,136,1230-1241.
[41] Xiaoli Chen & Ruijuan Hu. (2025). Intelligent English multiple-choice question scoring method based on LeNet-5 and strengthened convolutional module. Systems and Soft Computing,7,200314-200314.
[42] Qiushuang Zheng,Hu Zhang,Hongbing Liu,Hao Xu,Bo Xu & Zhenhao Zhu. (2025). Intelligent prediction model for pitting corrosion risk in pipelines using developed ResNet and feature reconstruction with interpretability analysis. Reliability Engineering and System Safety,264(PA),111347-111347.